Characterization of Two Membrane-Bound Forms of OmpA†

Natalia A. Rodionova,‡,§ Suren A. Tatulian,‡ Thomas Surrey,|| Fritz Jähnig,|| and Lukas K. Tamm*,‡

Department of Molecular Physiology and Biological Physics, University of Virginia School of Medicine, Health Sciences Center, Box 449, Charlottesville, Virginia 22908, and Abteilung Membranbiochemie, Max-Planck-Institut für Biologie, Corrensstrasse 38, D-72076 Tübingen, Germany

Received July 15, 1994; Revised Manuscript Received November 1, 1994⊗

ABSTRACT: The insertion of the outer membrane protein A (OmpA) into lipid bilayers was studied by limited proteolysis, polarized Fourier transform infrared (FTIR) spectroscopy, and fluorescence spectroscopy. In the native state, OmpA is thought to form a barrel of eight antiparallel β-strands. For the present study, it was isolated in an unfolded form, purified, and exposed to preformed vesicles of 1-palmitoyl-2-oleoyl-phosphatidylcholine (POPC), dimyristoylphosphatidylcholine (DMPC), dipalmitoylphosphatidylcholine (DPPC), and three phospholipids that were brominated in different positions of their *sn*-2 chains (4,5-BrPC, 9,10-BrPC, and 11,12-BrPC). Limited proteolysis revealed two membrane-bound forms of OmpA, namely an "adsorbed" (35 kDa) and an "inserted" (30 kDa) form [Surrey, T., & Jähnig, F. (1992) *Proc. Natl. Acad. Sci. U.S.A. 89*, 7457−7461]. Which form was found after membrane binding and refolding depended on the lipids used and on the temperature. Polarized attenuated total reflection (ATR)-FTIR spectra were recorded with OmpA bound to germanium-supported bilayers in both forms. The position of the amide I′ band indicated quite large fractions of β-structure of OmpA in both membrane-bound forms (35−45% in the adsorbed form and 45−55% in the inserted form). Measurements of the linear dichroism of the amide I′ bands in the inserted form are consistent with an antiparallel β-barrel in which the strands are inclined at about 36° from the membrane normal. The average angle of the β-strands to the bilayer normal is likely larger in the 35 kDa form than in the inserted form. The extent of quenching of the tryptophan fluorescence in the presence of brominated lipids depended on the position of the bromines in the fatty acyl chain. In the inserted form, 4,5-BrPC quenched the fluorescence most efficiently, which indicates an average location of the tryptophan residues close to the bilayer surface. In the 35 kDa form, tryptophan fluorescence was most efficiently quenched by 9,10-BrPC, which indicates a partial insertion of these residues in the hydrophobic part of the bilayer. Fluorescence spectroscopy in the presence of the soluble quencher acrylamide showed that after binding to the membrane the five tryptophan residues of OmpA are protected from the aqueous environment to a similar extent in both forms.

There are probably two key reasons for our current lack of knowledge in the area of membrane protein folding: (1) Only a few atomic structures of integral membrane proteins are known, and (2) most membrane proteins require detergents for their solubilization, which are difficult to remove in a direct refolding experiment. The second limitation has been overcome for the case of the outer membrane protein A (OmpA),[1] because this protein can be completely unfolded in urea (Schweizer et al., 1978) and has recently been found to spontaneously refold and insert into lipid bilayers upon rapid dilution of urea (Surrey & Jähnig, 1992). This property, plus its similarity to the bacterial porins of which four crystal structures are known (Weiss et al., 1991; Cowan et al., 1992; Kreusch et al., 1994), makes OmpA a preferred model for studying the mechanism of integral membrane protein folding.

OmpA is one of the major proteins of the outer membrane of *Escherichia coli*. The sequence of the single polypeptide chain of OmpA is known and consists of 325 amino acids (Chen et al., 1980). The electrophoretically determined apparent molecular mass of the protein after boiling in SDS is about 35 kDa and about 30 kDa without the heat treatment (Schweizer et al., 1978). When OmpA is digested with trypsin in its native membrane environment, a 24 kDa fragment is generated, which constitutes the N-terminal membrane-protected part of the protein. This domain is predicted to span the membrane in eight antiparallel β-strands, which presumably form a β-barrel (Vogel & Jähnig, 1986). Several functions have been attributed to OmpA: Together with lipopolysaccharide, OmpA constitutes the receptor for phage TuII and F-mediated conjugation (Van Alphen, 1977); OmpA is required for the action of a colicin (Chai & Foulds, 1974); and in combination with the outer membrane lipoprotein, OmpA is responsible for the generation of normal cell shape (Sonntag et al., 1978).

Previous studies showed that OmpA that was unfolded by urea can be refolded by removal of the denaturant in the

†Supported by NIH Grant R01 AI30557 to L.K.T.

* Corresponding author.

‡ University of Virginia School of Medicine.

§ Permanent address: Institute of Cell Biophysics, Russian Academy of Sciences, Pushchino, Moscow Region, 142292 Russia.

|| Max-Planck Institut für Biologie.

⊗ Abstract published in *Advance ACS Abstracts,* January 15, 1995.

[1] Abbreviations: ATR, attenuated total reflection; *n,n′*-BrPC, 1-palmitoyl-2-stearoyl(dibromo)phosphatidylcholine (labeled at positions *n* and *n′*); CD, circular dichroism; DMPC, dimyristoylphosphatidylcholine; DPPC, dipalmitoylphosphatidylcholine; FTIR, Fourier transform infrared; HEPES, *N*-(2-hydroxyethyl)piperazine-*N′*-2-ethanesulfonic acid; MES, 2-(*N*-morpholino)ethanesulfonic acid; OmpA, outer membrane protein A; POPC, 1-palmitoyl-2-oleoylphosphatidylcholine; TLCK, N^{α}-*p*-tosyl-L-lysine chloromethyl ketone.

0006-2960/95/0434-1921$09.00/0

presence of phospholipid vesicles (Surrey & Jähnig, 1992). Moreover, OmpA was found to be bound to the vesicles in two different forms, which depended on the state of the constituent phospholipids. When fluid lipid bilayers (DMPC at 30 °C) were used in refolding experiments as target vesicles, OmpA inserted into those vesicles presumably in its native form, because the CD spectra indicated a similar content of β-structure after refolding as in the native form, the apparent molecular mass was changed after refolding to the native 30 kDa form in SDS gels, and the characteristic 24 kDa fragment was found after trypsin digestion. However, when OmpA was refolded in the presence of solid lipid bilayers (DMPC at 15 °C), it produced a band on SDS gels at 35 kDa, which is typical for unfolded OmpA, and it was completely digested by trypsin. The secondary structure and the changes in tryptophan fluorescence were very similar in the two membrane-bound forms. Therefore, it was concluded that OmpA was "adsorbed" to the surface of DMPC vesicles at 15 °C. In the present study, we further characterize these two membrane-bound forms of OmpA. As experimental techniques, we use polarized attenuated total reflection (ATR) Fourier transform infrared (FTIR) spectroscopy and fluorescence spectroscopy in conjunction with soluble and membrane-bound quenchers. We find that the "adsorbed" (35 kDa) form may actually be partially inserted into the bilayer and that the antiparallel strands of the β-pleated sheets become reoriented when OmpA is completely inserted into the bilayer.

MATERIALS AND METHODS

Materials. OmpA was isolated and purified from outer membranes of *E. coli* using the procedure described by Surrey and Jähnig (1992). 4,5-BrPC was kindly provided by Dr. P. W. Holloway (Department of Biochemistry, University of Virginia). All other lipids were from Avanti Polar Lipids (Alabaster, AL). Acrylamide (ultra-pure grade) for fluorescence quenching and all other biochemicals were from Sigma (St. Louis, MO).

Preparation of Small Unilamellar Lipid Vesicles. Phospholipids (about 10 mg) in chloroform were dried on the bottom of a glass test tube under a stream of dry nitrogen. All membranes with brominated lipids were a mixture of DMPC and *n,n'*-BrPC at a molar ratio of 4:1. Then the lipids were dried in a high vacuum for 1 h and dispersed at a concentration of 3 mM by vigorous vortexing in 20 mM sodium phosphate buffer, pH 7.3, containing 0.15 M NaCl. Small unilamellar vesicles were prepared by pulsed sonication with a microtip sonifier for 30 min. The temperature was maintained in a water bath at room temperature, except for DPPC, which was kept at 45 °C. The vesicles were left to equilibrate overnight above their respective phase transition temperatures prior to their use.

Reconstitution and Refolding. OmpA was reconstituted into the preformed vesicles by oriented insertion as described (Surrey & Jähnig, 1992). A small volume of unfolded protein at a concentration of 2 mg/mL (8 mg/mL for gel electrophoresis) in 8 M urea was added to the vesicles (0.5–0.6 mM lipid for fluorescence and FTIR spectroscopy, 3 mM for gel electrophoresis) to give molar lipid-to-protein ratios of about 800 for the fluorescence, 600 for the FTIR, and 300 for the gel electrophoresis experiments. The samples were analyzed after incubation at the appropriate temperature and completion of adsorption or insertion, i.e., typically after 1 h for vesicles below, and after 4 h for vesicles above their respective lipid phase transition temperature. Kinetic experiments using fluorescence spectroscopy showed that these times were sufficient for binding of OmpA to the lipid bilayers (unpublished results). Due to some protein aggregation at pH 7.3, the yield of the reconstitution varies between 60% and close to 100% depending on the protein concentration. The higher yields are obtained for the lower protein concentrations such as those used for the FTIR and fluorescence measurements.

SDS–Polyacrylamide Gel Electrophoresis and Trypsin Digestion. SDS–PAGE was performed on 12% polyacrylamide gels with 0.1% SDS in the running buffer (Laemmli, 1970). The samples were not boiled. The gels were stained with Coomassie brilliant blue R-250 as described by Weber and Osborn (1964). Samples were digested with trypsin (Sigma; type XIII, TPCK-treated) at a molar enzyme-to-substrate ratio of 1:200. Digestion was stopped by addition of TLCK at a molar ratio of trypsin to inhibitor of 1:250.

Supported Planar Lipid Bilayers and ATR-FTIR Spectroscopy. Supported planar bilayers were prepared from the vesicles with bound OmpA by the monolayer fusion technique as described previously (Kalb et al., 1992; Frey & Tamm, 1991; Tamm & Tatulian, 1993). In this technique, the OmpA vesicles in 20 mM sodium phosphate buffer (pH 7.3)/0.15 M NaCl were allowed to fuse to a supported monolayer of the same lipid as that used for the vesicles. The monolayer was first deposited on a germanium plate by the Langmuir–Blodgett technique. After fusion of the vesicles was complete (about 60 min), the buffer was exchanged in the ATR sample cell with 10 volumes of 5 mM HEPES/10 mM MES buffer, pH 7.2, prepared in D_2O and containing 135 mM NaCl. In addition to exchanging H_2O for D_2O, this step washes away residual noninserted protein and lipid. This method produces single supported bilayers with a very similar lipid phase behavior and lipid dynamic properties as measured in more conventional vesicle or multibilayer systems (Kalb et al., 1992; Frey & Tamm, 1991). About 1 h elapsed after the H_2O/D_2O exchange and before the first FTIR spectrum was recorded on a Nicolet 740 FTIR spectrometer as described (Tamm & Tatulian, 1993). A total of 2 000 scans were collected at each polarization with a spectral resolution of 2 cm^{-1}. The transmittance spectra were ratioed with reference scans obtained from pure D_2O buffer in the ATR cell. All experiments were carried out at room temperature (21 + 2 °C). The spectra were analyzed on a personal computer using the LabCalc program (Galactic Industries, Salem, NH). Second-derivative spectra were calculated by differentiation with an 11-point Savitsky–Golay smoothing. Spectral decomposition was carried out by a least-squares fitting procedure using Gaussian component line shapes. The ATR dichroic ratios of the amide I' bands were calculated from the integrated component band intensities according to

$$R^{\mathrm{ATR}}_{\mathrm{amide\ I}} = \frac{\int A_{\parallel}(\nu)\,\mathrm{d}\nu}{\int A_{\perp}(\nu)\,\mathrm{d}\nu} \qquad (1)$$

where $A_{\parallel}(\nu)$ and $A_{\perp}(\nu)$ are the absorbances at frequencies ν with the electric vector of the infrared beam polarized parallel and perpendicular to the plane of incidence, respec-

tively [for definitions, see Frey and Tamm (1991)]. The ATR dichroic ratios of the methylene stretching vibrations of the lipids in the supported bilayers were calculated as $R_L^{ATR} = A_{||}(\nu_{max})/A_{\perp}(\nu_{max})$, where ν_{max} values are the peak wavenumbers of the symmetric or antisymmetric methylene stretching vibrations.

Order Parameters and Lipid-to-Protein Ratios. The experimental parameter obtained from a dichroic measurement is the order parameter which is defined as

$$S_\theta = (3\langle\cos^2\theta\rangle - 1)/2 \quad (2)$$

where θ is the angle between the axis of rotational symmetry of an axially symmetric molecule (long axis of the lipid, α-helix, β-barrel, etc.) and the normal to the germanium plate and the angular brackets denote a time and space average over all angles in a given sample. The lipid order parameter is calculated from the experimental dichroic ratio using the relation (Fringeli & Günthardt, 1981; Frey & Tamm, 1991):

$$S_L = -2\frac{E_x^2 - R_L^{ATR}E_y^2 + E_z^2}{E_x^2 - R_L^{ATR}E_y^2 - 2E_z^2} \quad (3)$$

where E_x, E_y, and E_z are the electric field amplitudes at the germanium−buffer interface. For the conditions used in this and our previous work, and ignoring possible small changes due to dispersion in the spectral region of interest, $E_x^2 = 1.9691$, $E_y^2 = 2.2486$, and $E_z^2 = 1.8917$ (Tamm & Tatulian, 1993). An order parameter S_Θ may also be defined analogous to eq 2 with respect to the angular distribution (angle Θ) of the transition dipole moments relative to the normal to the germanium plate. This order parameter for an amide I band component is:

$$S_{\text{amide I}} = \frac{E_x^2 - R_{\text{amide I}}^{ATR}E_y^2 + E_z^2}{E_x^2 - R_{\text{amide I}}^{ATR}E_y^2 - 2E_z^2} \quad (4)$$

The lipid-to-protein molar ratios of the supported planar bilayers can be determined from Beer−Lambert's law modified for polarized ATR spectroscopy. The relevant equation is (Tamm & Tatulian, 1993)[2] :

$$L/P = 0.208(n_{res} - 1)\frac{1 - S_{\text{amide I}}}{1 + S_L/2}\frac{\int_{2800}^{2980}A_{\perp}(\nu_L)\,d\nu}{\int_{1600}^{1690}A_{\perp}(\nu_{\text{amide I}})\,d\nu} \quad (5)$$

where n_{res} is the number of residues in the polypeptide and ν_L and $\nu_{\text{amide I}}$ are the wavenumbers of the lipid methylene stretch and the protein amide I vibrations, respectively.

Fluorescence Spectroscopy. Fluorescence measurements were performed on a SPEX spectrofluorometer (SPEX Industries, Edison, NJ). The vesicle suspensions with OmpA were stirred in a 1.0 × 0.4 cm temperature-controlled quartz cuvette. The protein and lipid concentrations were kept at 0.6−0.8 μM and 0.6 mM, respectively, throughout this study. The tryptophan emission spectra were recorded with excitation at 290 nm; 4.25 nm bandwidths were used in both the excitation and emission pathways. The fluorescence intensities were corrected for dilution factors and light scattering.

[2] To arrive at eq 5 from eq A4 of Tamm and Tatulian (1993), it is recognized that $\sigma_1 = (1+ S_L/2)/3$ and $\sigma_2 = (1- S_{\text{amide I}})/3$.

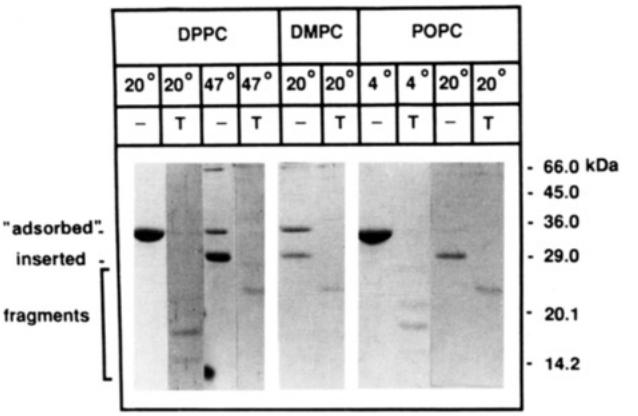

FIGURE 1: SDS−polyacrylamide gel demonstrating binding and insertion of OmpA with vesicles of DPPC, DMPC, and POPC at various temperatures. Samples of OmpA were incubated with the vesicles at the indicated temperatures. The samples in the lanes marked with T were digested with trypsin after binding to the vesicles and at the indicated temperatures. The samples were not boiled in SDS.

Backgrounds of light scattering were determined with vesicles of identical composition and concentration, but in the absence of protein.

RESULTS

Binding and Insertion into Preformed Vesicles. OmpA was isolated in an unfolded form and bound at various temperatures to preformed small unilamellar vesicles of DPPC, DMPC, and POPC, which undergo chain melting phase transitions at 41, 24, and about −4° C, respectively. Figure 1 shows SDS gels of OmpA bound to DPPC, DMPC, and POPC at various temperatures. At 20 °C, OmpA bound to DPPC vesicles in the 35 kDa from and to POPC vesicles in the 30 kDa form, but both forms were found when OmpA was bound to DMPC vesicles at this temperature. The 30 kDa form was digested by trypsin to a single fragment of 24 kDa. This cleavage is characteristic for the membrane-inserted form of OmpA (Schweizer et al., 1978). In contrast, the 35 kDa form was essentially degraded completely by trypsin. If the gels are run at high protein content, two fragments with apparent molecular masses of 18 and 15 kDa remain detectable. They represent fragments of the C-terminal periplasmic part of OmpA, because they never appear when the 24 kDa membrane-protected fragment is used to perform the experiment (Surrey and Jähnig, unpublished results). The essentially degradable form of OmpA was previously identified when the protein was bound to DMPC vesicles at 15° C and has been termed the "adsorbed" form (Surrey & Jähnig, 1992). When OmpA was bound to DPPC vesicles at 47 °C, the predominant form was the inserted form as expected for membranes in the liquid-crystalline (fluid) phase (Figure 1). However, OmpA bound to POPC vesicles at 4° C exclusively in the 35 kDa form, which was degraded by limited trypsin digestion to three fragments of 21, 18, and 15 kDa, respectively (Figure 1). This latter result is interesting because POPC bilayers at 4 °C are most likely in the liquid-crystalline phase.[3]

[3] The chain melting phase transition temperature of POPC has been measured to occur at −5 to −3 °C by various authors and techniques (de Kruijff et al., 1973; Perly et al., 1985; Lynch & Steponkus, 1989), although a value of +4 °C has also been reported (Barenholz et al., 1976).

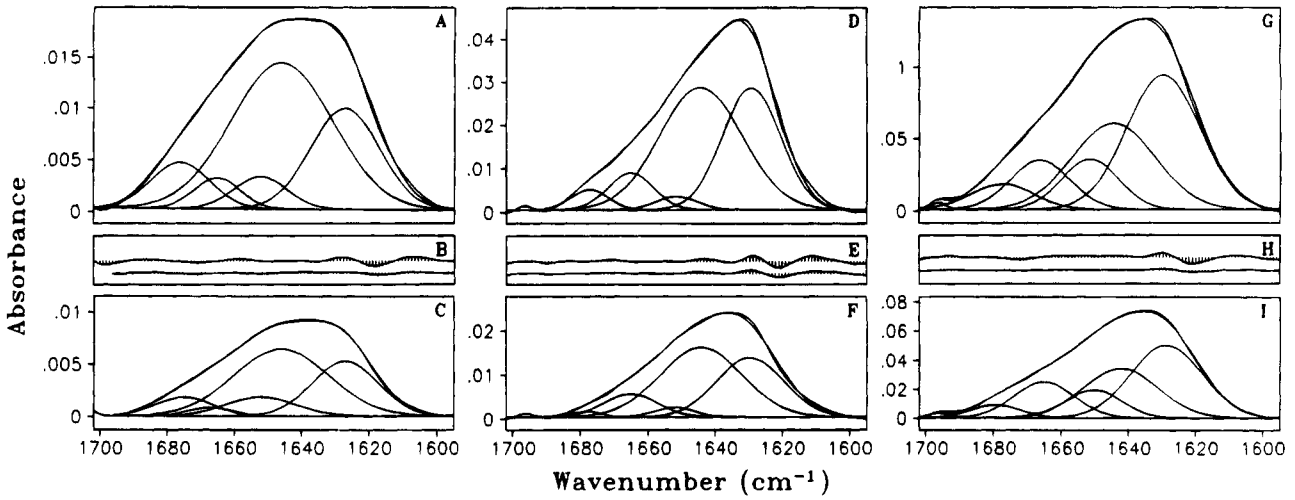

FIGURE 2: Polarized ATR-FTIR spectra of OmpA bound to supported planar bilayers of DPPC (panels A−C), DMPC (panels D−F), and POPC (panels G−I) in the amide I′ region. The spectra of the upper panels were recorded with parallel polarized light and those of the lower panels with perpendicular polarized light. The results of spectral decompositions with six Gaussian components are also shown in the upper and lower panels. The differences between the experimental and summed component band spectra are displayed in panels B, E, and H. The spectra for each lipid are normalized to a common absorbance scale.

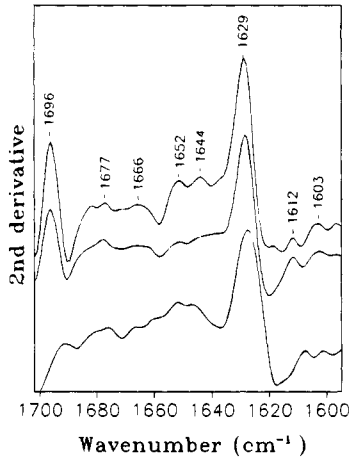

FIGURE 3: Second-derivative spectra of the paralled polarized amide I′ spectra shown in Figure 2, indicating the positions of the component bands in POPC (top), DMPC (middle), and DPPC (bottom). The spectra were inverted along the ordinate to facilitate the identification of the component peaks.

Table 1: Results of the Six-Component Spectral Decompositions of the Polarized ATR-FTIR Spectra of OmpA Bound to Planar Bilayers of DPPC, DMPC, and POPC

	wavenumber (cm^{-1})		relative band area (%)	
lipid	parallel	perpendicular	parallel	perpendicular
DPPC	1627, 1676[a]	1627, 1675[a]	35	37
	1646	1646	54	50
	1652	1652	6	10
	1665	1667	4	3
	1691	1689	<1	<1
DMPC	1629, 1677[a]	1629, 1678[a]	39	36
	1644	1644	50	50
	1651	1652	3	3
	1664	1665	8	11
	1696	1696	<1	<1
POPC	1629, 1677[a]	1629, 1679[a]	47	44
	1644	1642	29	28
	1651	1650	12	12
	1665	1665	12	15
	1696	1696	<1	<1

[a] The fractional band areas of these two peaks are summed, because they both contribute and are assigned to antiparallel β-sheet.

ATR-FTIR Spectroscopy. To determine the secondary structure of OmpA in both membrane-bound forms, we measured polarized ATR-FTIR spectra of OmpA bound to supported planar lipid bilayers. Our liquid ATR sample cell cannot be temperature-controlled. Therefore, we performed the FTIR measurements at room temperature with OmpA bound to supported planar bilayers of DPPC, POPC and DMPC. This corresponds to OmpA in the "adsorbed" and inserted and a mixture of these two forms, respectively (Figure 1). The amide I′ regions of representative ATR-FTIR spectra of OmpA bound to the three different lipid bilayers are shown in Figure 2. The amide I′ band of proteins is in general a composite band, representative of the different secondary structures in the protein. A common technique for identifying the peak wavenumbers of the component bands is to calculate second-derivative spectra of the amide I′ envelope (Susi & Byler, 1986; Arrondo et al., 1993). Figure 3 shows the second-derivative spectra of the parallel polarized amide I′ bands of OmpA bound to bilayers of DPPC, DMPC, and POPC. The most prominent peak occurs at 1627−1629 cm^{-1} in all spectra. Bands in this region are attributed to β-structure with practically no spectral overlap from other secondary structure components (Krimm & Bandekar, 1986; Susi & Byler, 1986; Arrondo et al., 1993). A weaker peak at 1676−1679 cm^{-1} indicative of antiparallel β-sheet is also found in all spectra. Other peaks that may be attributed to turns, α-helix, and random coil appear in the second-derivative spectra. However, their assignment is less certain than that of the low-frequency β-structure component.

To quantitate the relative contributions of the different components, especially that of the β-structure, the amide I′ contours were fitted with six component bands. In these fits, the wavenumber positions of the component bands were kept fixed at the positions that were identified in the derivative spectra. The results of these fits are shown in Figure 2 along with the original spectra. Table 1 summarizes the numerical values for all component bands of the spectra shown in Figure 2. The component bands at ~1629 and ~1677 cm^{-1} were previously shown to result from transition dipole coupling interactions of the amide I vibrations of an

Table 2: Wavenumbers, Dichroic Ratios, and Order Parameters of the Symmetric and Antisymmetric Lipid Methylene Stretching Vibrations in the Presence of "Adsorbed" or Inserted OmpA

lipid	band	ν (cm^{-1})	R_L^{ATR}	S_L
DPPC	symm	2850.4 ± 0.2	1.34 ± 0.02	0.35 ± 0.02
	antisymm	2918.4 ± 0.2	1.30 ± 0.03	0.40 ± 0.03
DMPC	symm	2851.9 ± 0.3	1.40 ± 0.03	0.29 ± 0.03
	antisymm	2921.8 ± 0.3	1.33 ± 0.05	0.36 ± 0.05
POPC	symm	2853.8 ± 0.3	1.53 ± 0.11	0.16 ± 0.10
	antisymm	2923.9 ± 0.2	1.42 ± 0.14	0.27 ± 0.14

antiparallel β-sheet (Miyazawa, 1960; Krimm & Abe, 1972). The higher-frequency component does not appear in the parallel β-sheet and is always weaker than the lower-frequency component in the antiparallel β-sheet (Miyazawa, 1960; Krimm & Abe, 1972). The very small, but distinct band at ~1696 cm^{-1} in POPC and DMPC may be due to a high-frequency component of antiparallel β-sheets or turns. The remaining bands at ~1644, ~1651, and ~1665 cm^{-1} could be due to random structure with incompletely H/D-exchanged amide protons, α-helix, and turns, respectively (Krimm & Bandekar, 1986; Susi & Byler, 1986; Arrondo et al., 1993), although their assignment is less certain (Surewicz et al., 1993). Assuming equal extinction coefficients for the amide I′ vibrations in all secondary structures (Krimm & Abe, 1972; Krimm & Bandekar, 1986), the relative content of β-structure in each spectrum may be estimated as the sum of the areas of the two peaks assigned to β-structure relative to the whole amide I′ area (Byler & Susi, 1986). Table 1 shows that OmpA "adsorbed" to DPPC forms ~36% β-structure, and ~45% β-structure was found when OmpA was inserted into POPC. The amount of β-structure found with DMPC is ~37%, i.e., intermediate between DPPC and POPC. Very similar relative contents of β-structure were found for each lipid in both polarizations which is a good indication that, at least in the case of OmpA, it is justified to deduce the amount of β-structure from the polarized spectra.

The absolute total areas of the β-components of the decomposed amide I′ bands at parallel and perpendicular polarization were ratioed to determine the ATR dichroic ratios of the β-structure, $R^{ATR}_{amide\ I}$. The $R^{ATR}_{amide\ I}$ values and the deduced order parameters $S_{amide\ I}$ are related to the orientation of the β-strands, as will be shown under Discussion. The mean $R^{ATR}_{amide\ I}$ values, averaged from three independent measurements in each case, were 2.07 ± 0.17, 1.81 ± 0.05, and 1.94 ± 0.04 for OmpA that was bound to bilayers of DPPC, DMPC, and POPC, respectively. The corresponding amide I order parameters were 0.123 ± 0.053, 0.036 ± 0.021, and 0.081 ± 0.015 for the three bilayers, respectively.

Information on the physical state of the lipids in the supported planar bilayer can be directly obtained from ATR-FTIR spectroscopy. The wavenumbers of the symmetric and antisymmetric methylene stretching vibrations increase upon melting of the lipid fatty acyl chains (Cameron et al., 1980). Chain melting is also accompanied by a small increase in the ATR dichroic ratios of the methylene stretching vibrations (Brauner et al., 1987; Hübner & Mantsch, 1991). Both of these effects are reproduced in the supported planar bilayers as shown in Table 2. In the presence of OmpA, the symmetric and antisymmetric stretching vibrations occur at about 2850 and 2918 cm^{-1} in DPPC, and increase by about 3−5 cm^{-1} in POPC bilayers. The average lipid order parameters decreased from about 0.38 to about 0.22 upon melting of the hydrocarbon chains. These values are comparable to those previously found in a similar system (Frey & Tamm, 1991). These data confirm that at room temperature DPPC is in the gel phase and POPC in the liquid-crystalline phase in the supported bilayers on the germanium plates, in excess water, and in the presence of bound OmpA. The corresponding experimental values for the DMPC bilayers are intermediate between those of DPPC and POPC and indicate that these bilayers are in the phase transition region at room temperature, which is consistent with our result that OmpA was only partially inserted into these membranes at 20 °C (Figure 1).

Table 3: Integrated Absorbances of the Methylene Lipid Stretching and Protein Amide I′ Absorbance Bands at Perpendicular Polarization and Deduced Lipid-to-Protein Ratios of OmpA Bound to Supported Lipid Bilayers

lipid	A_{lipid}[a]	$A_{amide\ I'}$[b]	L/P[c] (mol/mol)
DPPC	3.91 ± 0.17	0.41 ± 0.02	480 ± 80
DMPC	2.48 ± 0.20	1.02 ± 0.07	143 ± 28
POPC	2.02 ± 0.40	2.65 ± 0.36	48 ± 19

[a] Integrated from 2800 to 2980 cm^{-1}. [b] Integrated from 1600 to 1690 cm^{-1}. [c] Calculated from eq 5 using the number of residues, n_{res} = 325.

The lipid-to-protein ratios in the supported bilayers were determined by measuring the integrated total band areas and by use of eq 5 (Table 3). It is seen that with identical protein and lipid concentrations in the incubation mixture, about 10 times less protein remained bound to the planar bilayers of DPPC than to those of POPC. It should be noted that we used only the β-strand component of the amide I bands for calculating the value of $S_{amide\ I}$ in eq 5. This is a good approximation because the lipid-to-protein ratios are not extremely sensitive to $S_{amide\ I}$. Even for extreme values of $S_{amide\ I}$ of −0.5 or +1.0, the errors of the resulting lipid-to-protein ratios do not exceed 24%.

Fluorescence Spectroscopy. The five tryptophans of OmpA are all contained in the N-terminal 24 kDa membrane fragment. It has been previously reported that the tryptophan fluorescence intensity is increased and its peak emission is blue-shifted when OmpA refolds and binds to DMPC vesicles at 15 or 30° C (Surrey & Jähnig, 1992). The positions of the tryptophan residues in the two membrane-bound forms of OmpA in the lipid bilayer are not well-known, although they have been predicted to be near the membrane surface (Vogel & Jähnig, 1986). Therefore, we attempted to determine the average positions of these tryptophans in both membrane-bound forms by using membrane-bound and soluble quenchers of tryptophan fluorescence. Brominated phosphatidylcholines in which the bromines are placed in several different positions along the *sn*-2 fatty acyl chain have been developed as yardsticks to localize the positions of tryptophans of membrane proteins within the bilayer (Leto et al., 1980; East & Lee, 1982; Markello & Holloway, 1985). The average positions of the bromine atoms in lipid bilayers are known from X-ray diffraction studies (McIntosh & Holloway, 1987; Wiener & White, 1991). To perform quenching experiments with the brominated lipids, it is first shown by SDS gel electrophoresis that the inclusion of 20 mol % of the various brominated phosphatidylcholines into small vesicles of DMPC does not affect the binding behavior of OmpA with these vesicles

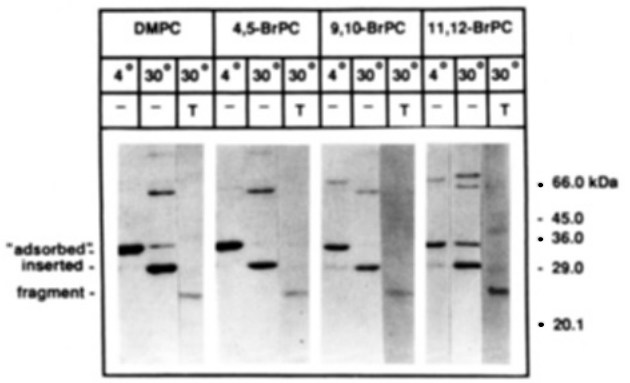

FIGURE 4: SDS−polyacrylamide gel demonstrating the binding and insertion of OmpA with vesicles of DMPC and DMPC containing 20 mol % of three different brominated lipids at 4 and 30 °C as indicated. The samples in the lanes marked with T were digested with trypsin after binding to the vesicles and at the indicated temperatures. The samples were not boiled in SDS.

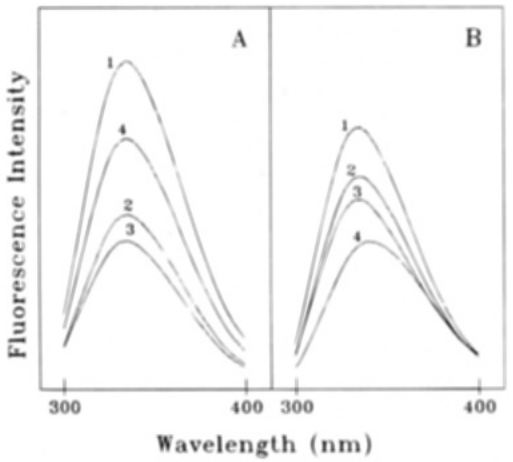

FIGURE 5: Fluorescence emission spectra of OmpA bound to vesicles of DMPC (1) and DMPC with 20 mol % 11,12-BrPC (2), 9,10-BrPC (3), and 4,5-BrPC (4) at 4 °C (panel A) and 30 °C (panel B). The relative fluorescence intensities were A1 = 100%, A2 = 76%, A3 = 53%, A4 = 45%, B1 = 100%, B2 = 81%, B3 = 73%, and B4 = 56%. The OmpA concentration was 0.6 μM, and the lipid-to-protein ratio was 820.

(Figure 4). OmpA bound to all vesicles at 4 °C in the 35 kDa form. At 30 °C, OmpA was folded (30 kDa band) and inserted into the membrane as shown by the appearance of the 24 kDa fragment after trypsin digestion. Except for a small amount of OmpA that remained in the 35 kDa form when 20 mol % 11,12-BrPC vesicles were used, insertion and folding of OmpA into DMPC vesicles was not affected by the presence of the brominated lipids.

Figure 5 shows fluorescence emission spectra of OmpA bound to small unilamellar vesicles of DMPC and DMPC with 20 mol % 4,5-BrPC, 20 mol % 9,10-BrPC, and 20 mol % 11,12-BrPC. At both temperatures, 4 and 30 °C, the bromines substantially decreased the tryptophan fluorescence intensities. Except for the vesicles with 4,5-BrPC at 30 °C where the fluorescence maximum occurred at 339 nm, the fluorescence maxima were all blue-shifted to 334−335 nm, indicating an apolar environment. Unfolded OmpA had a fluorescence maximum at 350 nm. At 30 °C, the relative fluorescence intensities decreased from 100% for DMPC to 81%, 73%, and 56% for 11,12-BrPC, 9,10-BrPC, and 4,5-BrPC vesicles, respectively. At 4 °C, however, the order of vesicles with decreasing relative fluorescence intensities was different: DMPC (100%), 4,5-BrPC (76%), 11,12-BrPC

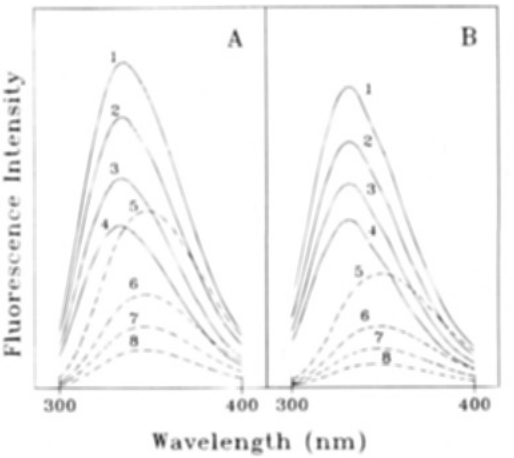

FIGURE 6: Tryptophan fluorescence quenching by acrylamide of OmpA in the unfolded and both membrane-bound forms. OmpA was bound to DMPC vesicles at 10 °C (panel A) and 30 °C (panel B), respectively. The lipid-to-protein ratio was 800. Spectra 5−8 were recorded in 4 M urea at the same respective temperatures and with the same concentrations of OmpA that were used for the membrane-bound samples (0.8 μM). The acrylamide concentrations were 0 (spectra 1 and 5), 0.12 M (spectra 2 and 6), 0.24 M (spectra 3 and 7), and 0.40 M (spectra 4 and 8).

(53%), 9,10-BrPC (45%). These data indicate that the tryptophans, on average, are closer to carbon numbers 4 and 5 than to carbon numbers 9−11 in the *sn*-2 chain of the phospholipids at 30 °C, but that they are more deeply buried in the membrane interior at 4 °C. Results similar to those at 4 °C were obtained when OmpA was bound to the various brominated vesicles at 10 °C (data not shown).

To determine whether (some of) these tryptophans were still accessible from the aqueous solution, quenching experiments were carried out with the soluble quencher acrylamide. These data are presented in Figure 6. In panel A, tryptophan quenching of membrane-bound OmpA in the 35 kDa form at 10 °C is compared to tryptophan quenching in the unfolded form in 4 M urea at this temperature. Large decreases of the fluorescence intensities were observed in both cases. Although the emission maximum of the membrane-bound form was 334 nm and that of the unfolded form was 350 nm, no spectral shifts were observed upon quenching by acrylamide in either form. Panel B shows the corresponding data for the membrane-inserted (30 kDa) form at 30 °C. Again, acrylamide quenched the fluorescence intensity in both forms, but did not change the emission maxima in either form (335 and 350 nm, respectively).

The data of Figure 6 and additional data at intermediate acrylamide concentrations are plotted as Stern-Volmer plots in Figure 7. Straight lines were obtained for both membrane-bound forms of OmpA. The Stern-Volmer quenching constants were calculated to be 2.8 and 2.2 M^{-1} for the 35 and 30 kDa forms, respectively. The dependency of F_0/F on the concentration of the quencher for OmpA in 4 M urea is steeper than for the membrane-bound forms, indicating that at least some of the tryptophan residues are protected by the membrane in both forms. Also, the Stern-Volmer plots of OmpA in 4 M urea are not linear which could be due to a static component to tryptophan quenching, in addition to the collisional component. Even though OmpA is fully denatured only at 8 M urea, all tryptophans are fully accessible at 4 M urea, because no changes of tryptophan fluorescence are observed between 4 and 8 M urea (Surrey

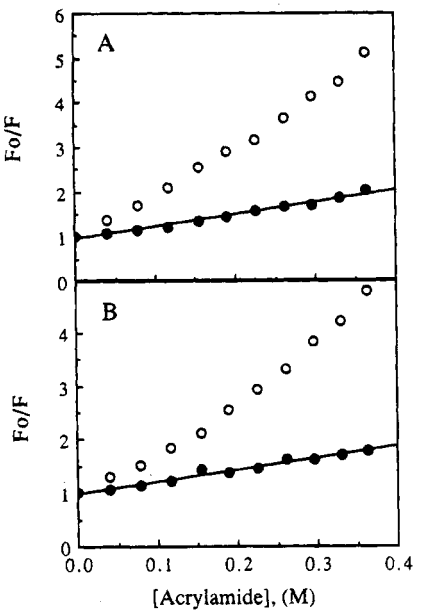

FIGURE 7: Stern-Volmer plots of OmpA in 4 M urea (●) or bound to DMPC vesicles (○) at 10 °C (panel A) and 30 °C (panel B). F_0 and F are the fluorescence intensities in the absence and presence of acrylamide, respectively. Straight lines with slopes of 2.8 and 2.2 M^{-1} are obtained for the membrane-bound samples at 10 and 30 °C, respectively.

& Jähnig, 1992) and because acrylamide quenched the tryptophan fluorescence to the same extent at 4 and 8 M urea (data not shown).

DISCUSSION

Secondary Structure. There is a large body of experimental evidence that OmpA forms an 8-stranded antiparallel β-sheet in the outer membrane of *E. coli* (Cole et al., 1983; Morona et al., 1984; Freudl et al., 1986; Vogel & Jähnig, 1986). It is likely that the β-strands are organized as a β-barrel in lipid bilayers with four antiparallel membrane-spanning loops of β-strand (Vogel & Jähnig, 1986). Therefore, OmpA is thought to be similar to the outer membrane porins of *R. capsulatus*, *E. coli*, and *R. blastica*, which exist as 16-stranded antiparallel β-barrels as recently shown by X-ray crystallography (Weiss et al., 1991; Cowan et al., 1992; Kreusch et al., 1994). A useful feature of OmpA is that it refolds from an unfolded form in urea in the presence of membranes and upon removal of the denaturant (Surrey & Jähnig, 1992). The FTIR experiments presented here demonstrate that the refolded and membrane-inserted form of OmpA in fluid membranes of POPC consists of a large fraction of β-structure (~45%). This is in reasonable agreement with Raman studies, which showed ~55% β-structure for native OmpA or OmpA that was reconstituted into *E. coli* lipopolysaccharide vesicles by detergent dialysis (Vogel & Jähnig, 1986). A significant amount of β-structure was also found by CD spectroscopy for refolded OmpA in DMPC vesicles at 30 °C (Surrey & Jähnig, 1992). When bound to solid membranes of DPPC, OmpA still forms a significant amount of β-structure (~36%). The relative amount of β-structure found depends to some extent on the fitting procedure used. If the main β-sheet components are centered at slightly (1−2 cm^{-1}) higher wavenumbers than those shown in the second derivatives (Figure 3), the quality of the fits improves, and considerably larger contents of β-sheet are obtained. Therefore, the percentages of β-sheet shown in Table 1 should be considered as lower limits, and we conclude that β-sheet contents up to about 45% (DPPC) and 55% (POPC) would also be consistent with our data. Because of these uncertainties and because the four central component peaks are rather weak in the derivative spectra, we attribute very little significance to their actual positions and did not derive secondary structures other than the β-sheet [for a critical assessment of secondary structure determination from FTIR spectroscopy, see Surewicz et al. (1993)]. We singled out the β-sheet component mainly for calculating the dichroic ratios of this component. We further found that the calculated dichroic ratios are quite insensitive to relatively large changes in the adopted band-fitting procedures, because the component bands scale by similar factors in the parallel and perpendicular polarized spectra.

Orientation. The dichroic ratios of the total β-structure component were used to gain insight into possible orientations of the β-strands relative to the membrane normal. Each ATR dichroic ratio is determined by the average orientations of the amide I transition dipole moments in a given sample. If the orientation of a transition moment relative to a particular axis of an element of secondary structure is known, the average orientation of that element of secondary structure relative to the plane of the membrane can be determined. Average orientations are commonly expressed in terms of order parameters, and the order parameter for the amide I band (angle Θ) may be calculated by eq 4. If the transition moments are distributed uniformly around a molecular symmetry axis and if the angle α between the transition moment and the molecular axis is known, $S_{\text{amide I}}$ can be converted into an order parameter describing the average orientation (in terms of angle θ) of that molecular axis relative to the bilayer normal. For example, for an α-helix α = 39° and the order parameter becomes

$$S_H = \frac{2S_{\text{amide I}}}{3\cos^2\alpha - 1} = 2.46S_{\text{amide I}} \qquad (6)$$

Insertion of eq 4 into eq 6 leads to the equation that we have previously used to determine order parameters of α-helices from ATR dichroic ratios (Frey & Tamm, 1991; Tamm & Tatulian, 1993).

The situation becomes more complex for evaluating order parameters of β-sheets, because in this case the transition moments are no longer uniformly distributed around any of the three principal axes of the sheet. It is known that the amide I transition moment is oriented close to parallel to the C=O bond of the amide group (Fraser & MacRae, 1973; Krimm & Bandekar, 1986). In a planar antiparallel β-sheet, the C=O bonds are oriented perpendicular to the strand direction and parallel to the plane of the β-sheet (Richardson, 1981). Therefore, measurement of an amide I order parameter does not yield a unique orientation of a β-sheet in the membrane, as indicated in Figure 8A. A second order parameter would be required to uniquely define the average orientation of a β-sheet in a bilayer. However, the following special cases may be considered. When $S_{\text{amide I}} = 1$, the C=O bonds are close to parallel to the membrane normal, and the sheet must run across the membrane with the strands oriented parallel to the plane of the membrane. When $S_{\text{amide I}} = -0.5$, the C=O bonds are oriented close to parallel to the plane of the membrane. This is the case, for example,

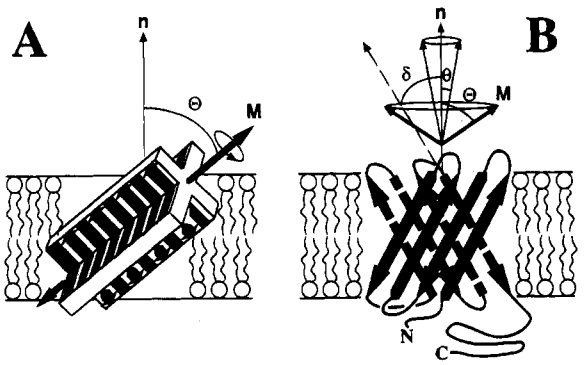

FIGURE 8: Models illustrating symmetry relations between β-sheets, their amide I transition dipole moments, and a planar lipid bilayer. *Panel A:* The orientation of planar antiparallel β-sheets is not uniquely determined by the angle Θ between the transition dipole moment M and the membrane normal n. The β-sheets can assume many orientations that are rotationally symmetric around M. Two orthogonal orientations are shown. When $\Theta = 0°$, the strands run parallel to the plane of the membrane, but adjacent strands of the sheet penetrate the membrane. When $\Theta = 90°$, the strands may run parallel to the plane of the membrane with alternating residues up and down, respectively, or they may be oriented parallel to the membrane normal. *Panel B:* The orientation of a β-barrel relative to the bilayer normal (angle θ) is determined by the angle Θ and the angle δ of the strands relative to the bilayer normal.

(1) for a sheet that is coplanar with the membrane, i.e., a situation expected for an amphiphilic β-sheet (or a single amphiphilic β-strand) with alternating polar and apolar residues (Kaiser & Kédzy, 1984), or (2) for a β-sheet with the strands crossing the membrane perpendicular to the membrane plane. Another interesting special case is that of an antiparallel β-barrel [for an example, see Cowan et al. (1992)]. Because this structure is axially symmetric, its orientation can be described with a single order parameter for the symmetry axis of the barrel, S_B. If the strands are inclined at an angle δ from the barrel axis (Figure 8B), the C=O bond angle to that axis is $90° - \delta$, and the angle of the amide I transition moment to the barrel axis is $\beta^{\pm} = 90° - \delta \pm \epsilon$, where ϵ is the angle between the amide I transition moment and the amide C=O bond. This angle is known to be ~20° (Fraser & MacRae, 1973; Krimm & Bandekar, 1986). Because the transition moment is always tilted toward the N $\rightarrow$ C_α direction and because in a β-strand alternating residues have their C=O bonds in opposite directions (180°), ϵ has to be added or subtracted for alternating residues, respectively. For porin, $\delta \approx 43°$ (Weiss et al., 1991; Cowan et al., 1992; Kreusch et al., 1994), $\beta^+ \approx 67°$, $\beta^- \approx 27°$, and

$$S_B = \frac{2S_{\text{amide I}}}{(3/2)(\cos^2\beta^+ + \cos^2\beta^-) - 1} = 4.76S_{\text{amide I}} \quad (7)$$

In a first model, we assume that OmpA in POPC forms a β-barrel similar to that of porin. We calculate S_B according to eq 7 from our experimental order parameter $S_{\text{amide I}} = 0.081$ and find the order parameter for the β-barrel to be 0.39. If this model of OmpA were correct, the β-barrel would be inclined from the bilayer normal at an average angle of 40°. Of course, the strands in an 8-stranded β-barrel such as OmpA may be inclined at a different angle than in a 16-stranded β-barrel such as the porins. Therefore, if we assume in a second model that the β-barrel is oriented with its long axis close to parallel to the membrane normal ($S_B \approx 1$), we may calculate from eq 7 the average angle δ that the strands would make relative to the barrel axis. In this model, we find $\delta \approx 36°$, which means that the strands in OmpA would run across the membrane at a somewhat steeper angle than in the porins. The amide I order parameter of the 35 kDa form of OmpA bound to bilayers of DPPC was 0.123. For this form, we have no reason to assume that OmpA forms a β-barrel even though the secondary structure seems similar as in the inserted form. The order parameter $S_{\text{amide I}}$ is larger for this form than for the inserted form. This means that the carbonyl groups, on average, are tilted more toward the membrane normal in the 35 kDa form than in the inserted form. Although, as shown above, average orientations of β-sheets are not uniquely defined by a single order parameter, our results could indicate that the strands on average are tilted more toward the membrane plane in the 35 kDa form than in the 30 kDa β-barrel form.

Location of Tryptophans in the Membranes. In the inserted form, the five tryptophans of OmpA on average are localized closer to the membrane surface than to the membrane center. This is evident from the larger quenching of the tryptophan fluorescence by 4,5-BrPC than by 9,10- or 11,12-BrPC. It is likely that the average tryptophan position is near the bromines of 4,5-BrPC at about 12−13 Å from the center plane of the bilayer (McIntosh & Holloway, 1987; Wiener & White, 1991). We have estimated this distance from our quenching data by the parallax method of Chattopadhyay and London (1987). This average position for the tryptophans in the inserted form of OmpA is in good qualitative agreement with the model of Vogel and Jähnig (1986), which locates most tryptophans near the membrane surface, i.e., about 15 Å from the center plane of the membrane. A location of the tryptophans near, but not at, the membrane surface is also borne out by the acrylamide quenching studies. At least some of the tryptophans are quenched by this soluble quencher, but the quenching efficiency (as expressed by the Stern-Volmer quenching constant) for the inserted form is much smaller than for the unfolded form of OmpA, indicating a partial shielding of the tryptophans from the aqueous phase.

Our quenching studies with the brominated lipids at 4 °C revealed that 9,10-BrPC was more effective in quenching the tryptophan fluorescence than 4,5- or 11,12-BrPC. Assuming that the lipid orientation is not altered due to adsorbed OmpA, these results indicate that the average position of the tryptophans is deeper in the membrane in the 35 kDa form than in the inserted form. The most likely position is about 7−8 Å from the center plane of the membrane, i.e., close to the approximate positions of the bromines in 9,10-BrPC (McIntosh & Holloway, 1987; Wiener & White, 1991). Therefore, these results argue against a strict surface location of the 35 kDa form of OmpA bound to gel-phase lipid membranes, and this form of OmpA may be better called a "partially inserted" than an "adsorbed" form. From our FTIR experiments, it is evident that most secondary structure is already formed in this form. The average orientation of the strands is likely more shallow in the partially inserted than in the fully inserted form. Because four of the five tryptophans have to cross the lipid bilayer in a refolding experiment [if we assume a topology of OmpA as predicted by Vogel and Jähnig (1986)], it is conceivable that the partially inserted, 35 kDa form of OmpA is a folding intermediate that is trapped by the gel-phase lipid, which

does not allow the β-loops to be translocated across the lipid bilayer.

ACKNOWLEDGMENT

We thank Dr. Peter Holloway for his kind gift of 4,5-BrPC.

REFERENCES

Arrondo, J. L. R., Muga, A., Castresana, J., & Goñi, F. M. (1993) *Prog. Biophys. Mol. Biol. 59*, 23−56.
Barenholz, Y., Suurkuusk, J., Mountcastle, D., Thompson, T. E., & Biltonen, R. L. (1976) *Biochemistry 15*, 2441−2447.
Brauner, J. W., Mendelsohn, R., & Prendergast, F. G. (1987) *Biochemistry 26*, 8151−8158.
Byler, D. M., & Susi, H. (1986) *Biopolymers 25*, 469−487.
Cameron, D., Casal, H., & Mantsch, H. (1980) *Biochemistry 19*, 3665−3672.
Chai, T., & Foulds, J. (1974) *J. Mol. Biol. 85*, 465−474.
Chattopadhyay, A., & London, E. (1987) *Biochemistry 26*, 39−45.
Chen, R., Schmidmayr, W., Krämer, C., Chen-Schmeisser, U., & Henning, U. (1980) *Proc. Natl. Acad. Sci. U.S.A. 77*, 4592−4596.
Cole, S. T., Chen-Schmeisser, U., Hindennach, I., & Henning, U. (1983) *J. Bacteriol. 153*, 581−587.
Cowan, S. W., Schirmer, T., Rummel, G., Steiert, M., Gosh, R., Pauptit, R. A., Jansonius, J. N., & Rosenbusch, J. P. (1992) *Nature 358*, 727−733.
deKruijff, B., Demel, R. A., Slotblom, A. J., van Deenen, L. L. M., & Rosenthal, R. F. (1973) *Biochim. Biophys. Acta 307*, 1−19.
East, J. M., & Lee, A. G. (1982) *Biochemistry 21*, 4144−4151.
Fraser, R. D. B., & MacRae, T. P. (1973) *Conformation in Fibrous Proteins and Related Synthetic Peptides*, pp 94−125, Academic Press, New York.
Freudl, R., MacIntyre, S., Degen, M., & Henning, U. (1986) *J. Mol. Biol. 188*, 491−494.
Frey, S., & Tamm, L. K. (1991) *Biophys. J. 60*, 922−930.
Fringeli, U. P., & Günthard, H. H. (1981) In *Membrane Spectroscopy* (Grell, E., Ed.) pp 270−332, Springer-Verlag, Berlin.
Hübner, W., & Mantsch, H. H. (1991) *Biophys. J. 59*, 1261−1272.
Kaiser, E. T., & Kézdy, F. J. (1984) *Science 223*, 249−255.
Kalb, E., Frey, S., & Tamm, L. K. (1991) *Biochim. Biophys. Acta 1103*, 307−316.
Ketchem, R. R., Hu, W., & Cross, T. A. (1993) *Science 261*, 1457−1460.
Kreusch, A., Neubüser, A., Schiltz, E., Weckesser, J., & Schulz, G. E. (1994) *Protein Sci. 3*, 58−63.
Krimm, S., & Abe, Y. (1972) *Proc. Natl. Acad. Sci. U.S.A. 69*, 2788−2792.
Krimm, S., & Bandekar, J. (1986) *Adv. Prot. Chem. 38*, 181−364.
Laemmli, U. K. (1970) *Nature 227*, 680−685.
Lakowicz, J. R. (1983) *Principles of Fluorescence Spectroscopy*, Plenum Press, New York.
Leto, T. L., Roseman, M. A., & Holloway, P. W. (1980) *Biochemistry 19*, 1911−1916.
Lynch, D. V., & Steponkus, P. L. (1989) *Biochim. Biophys. Acta 984*, 267−272.
Markello, T., Zlotnick, A., Everett, J., Tennyson, J., & Holloway, P. W. (1985) *Biochemistry 24*, 2895−2901.
McIntosh, T. J., & Holloway, P. W. (1987) *Biochemistry 26*, 1783−1788.
Miyazawa, T. (1960) *J. Chem. Phys. 32*, 1647−1652.
Morona, R., Klose, M., & Henning, U. (1984) *J. Bacteriol. 159*, 570−578.
Perly, B., Smith, I. C. P., & Jarrell, H. (1985) *Biochemistry 24*, 1055−1063.
Richardson, J. S. (1981) *Adv. Prot. Chem. 34*, 167−330.
Schweizer, M., Hindennach, M., Garten, W., & Henning, U. (1978) *Eur. J. Biochem. 82*, 211−217.
Sonntag, I., Scharc, H., Hirota, Y., & Henning, U. (1978) *J. Bacteriol. 136*, 280−285.
Surewicz, W., Mantsch, H. H., & Chapman, D. (1993) *Biochemistry 32*, 389−394.
Surrey, T., & Jähnig, F. (1992) *Proc. Natl. Acad. Sci. U.S.A. 89*, 7457−7461.
Susi, H., & Byler, D. M. (1986) *Methods Enzymol. 130*, 290−311.
Tamm, L. K., & Tatulian, S. A. (1993) *Biochemistry 32*, 7720−7726.
Van Alphen, L., Havekes, L., & Lugtenberg, B. (1977) *FEBS Lett. 75*, 285−290.
Vogel, H., & Jähnig, F. (1986) *J. Mol. Biol. 190*, 191−199.
Weber, K., & Osborn, M. (1964) *J. Biol. Chem. 244*, 4406−4412.
Weiss, M. S., Kreusch, A., Schiltz, E., Nestel, U., Welte, W., Weckesser, J., & Schulz, G. E. (1991) *FEBS Lett. 280*, 379−382.
Wiener, M. C., & White, S. H. (1991) *Biochemistry 30*, 6997−7008.

BI941604G